

# Semidiurnal write-up (Rough)

Kurtis Anstey

V00939802

Department of Physics and Astronomy

University of Victoria

July 20, 2021

Dr. Jody Klymak (University of Victoria)

Dr. Steven Mihaly (Ocean Networks Canada)

Dr. Richard Thomson (Institute of Ocean Sciences)

## Table of Contents

List of Figures	3
1 Observations	4
2 Comparisons	10
3 Speculation	10
4 Discussion	10
5 References	11

## List of Figures

1	Power spectra - 2013 . . . . .	4
2	Rotary spectra - 2013l . . . . .	5
3	Depth-frequency PSD - Tidal - 2013 . . . . .	6
4	Depth-frequency rotary spectra - Tidal - 2013 . . . . .	6
5	Depth-band PSD - Semidiurnal - 2013 . . . . .	7
6	Depth-band rotary PSD - Semidiurnal - 2013 . . . . .	8
7	Barotropic comparison - Semidiurnal - 2013 . . . . .	9

# 1 Observations

Spectra for both sites show strong semidiurnal influence, with little to no inter-annual variability (*Appendix A will show inter-annual comparisons*).

One of the primary tidal frequency constituents present at Barkley Canyon, the semidiurnal peak ( $2.22 \times 10^{-5}$  Hz) dominates the spectra (Figures 1 and 2).

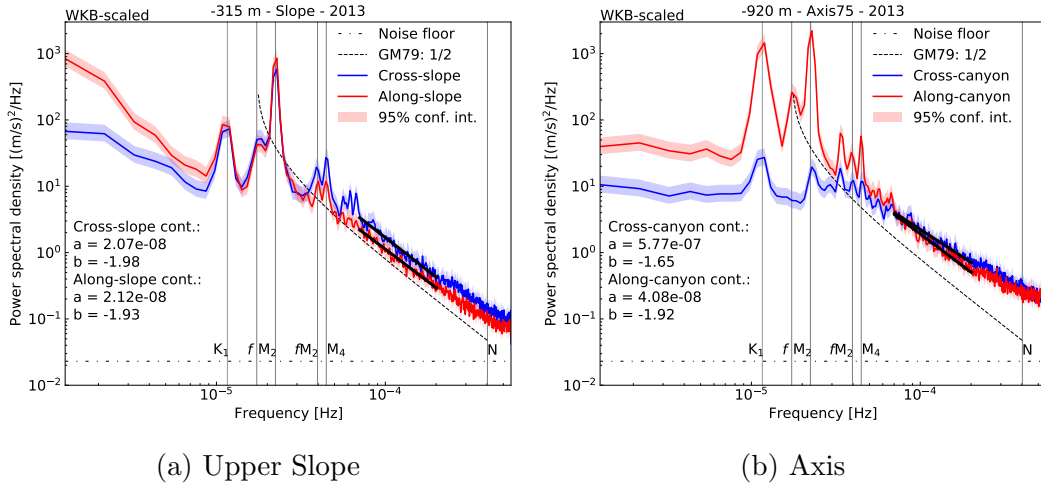


Figure 1: Time-mean PSD for (a) Upper Slope (-315 m) and (b) Axis (-920 m), from horizontal velocity data in 2013. Both cross- (blue) and along-slope/canyon (red) components are shown for comparison, with 95% confidence intervals. Solid black lines show continuum slope. For reference, the instrument noise floor (dotted line), component-wise GM79 spectrum (dashed line), and key frequency constituents (vertical lines) are shown.

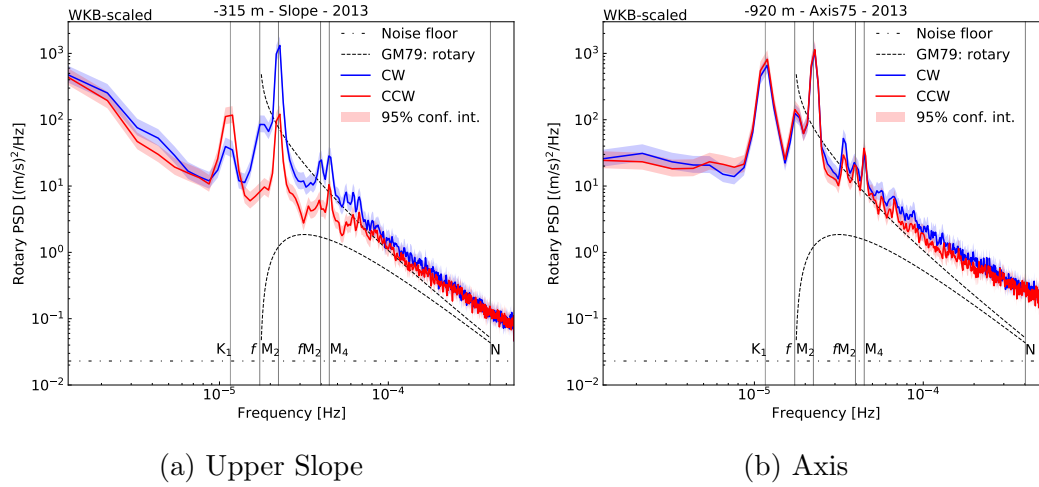


Figure 2: Time-mean rotary spectra for (a) Upper Slope (-315 m) and (b) Axis (-920 m), from horizontal velocity data in 2013. Both CW (blue) and CCW (red) components are shown for comparison, with 95% confidence intervals. For reference, the instrument noise floor (dotted line), rotary GM79 spectrum (dashed lines), and key frequency constituents (vertical lines) are shown.

From near-topography inter-annual power spectra at Upper Slope, the semidiurnal peak is strongly CW and equally distributed between cross- and along-slope components.

At Axis, the peak is rectilinear, and strongly along-canyon.

At both sites the total strength of the peak is on of the order of  $10^3 \text{ (m/s)}^2/\text{Hz}$ .

To better identify depth-dependence, spectra were computed at each depth (Figures 3 and 4).

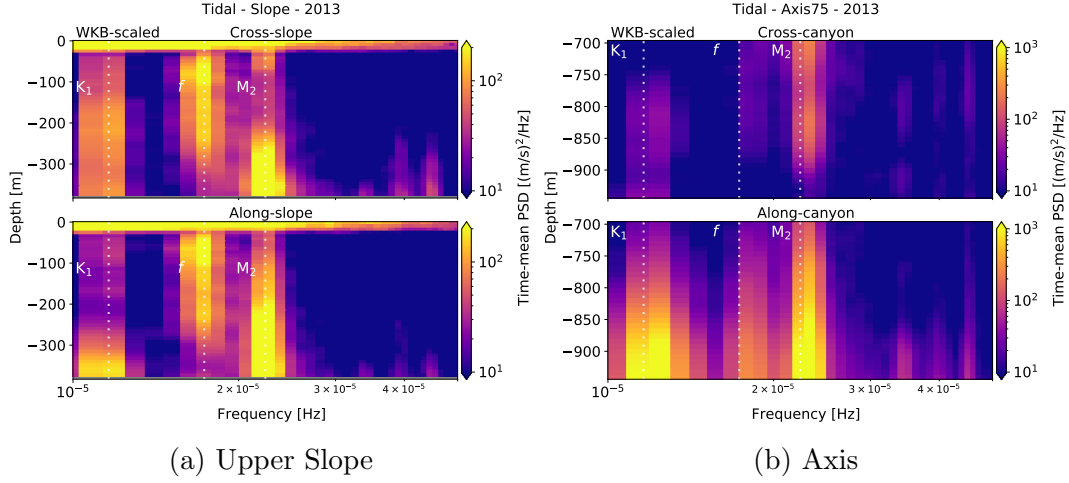


Figure 3: Depth-frequency PSD for (a) Upper Slope and (b) Axis, from horizontal velocity data in 2013. Frequency range has been truncated to better show the primary tidal constituents, noted as vertical dashed lines. Colour-bar scales (PSD) have been adjusted by site.

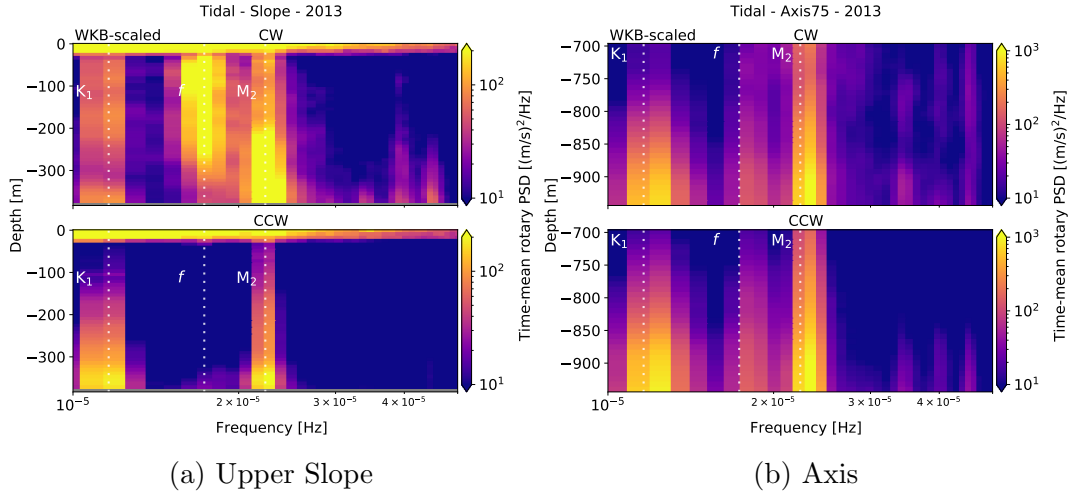


Figure 4: Depth-frequency rotary spectra for (a) Upper Slope and (b) Axis, from horizontal velocity data in 2013. Frequency range has been truncated to better show the primary tidal constituents, noted as vertical dashed lines. Colour-bar scales (rotary PSD) have been adjusted by site.

Qualities of the semidiurnal band are as noted in the specific depth spectra, but also show intensification near topography.

At Upper Slope, intensification is of an order of magnitude, and a vertical scale of about 150 m above bottom (AB).

At Axis, intensification is of nearly two orders of magnitude, and reaches about 250 m AB.

To observe potential seasonality, depth-frequency spectra were integrated across the approximate width of the semidiurnal peak ( $2.17 - 2.38 \times 10^{-5}$  Hz) to obtain 'depth-band integrated power' estimates for each spectral window (Figures 5 and 6), and plotted through time.

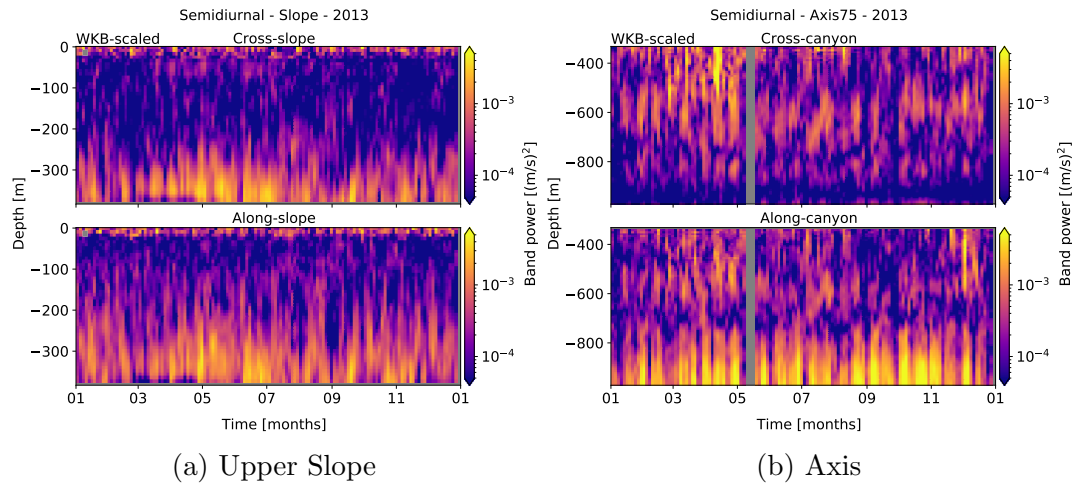


Figure 5: Integrated semidiurnal depth-band PSD for (a) Upper Slope and (b) Axis, from horizontal velocity data in 2013.

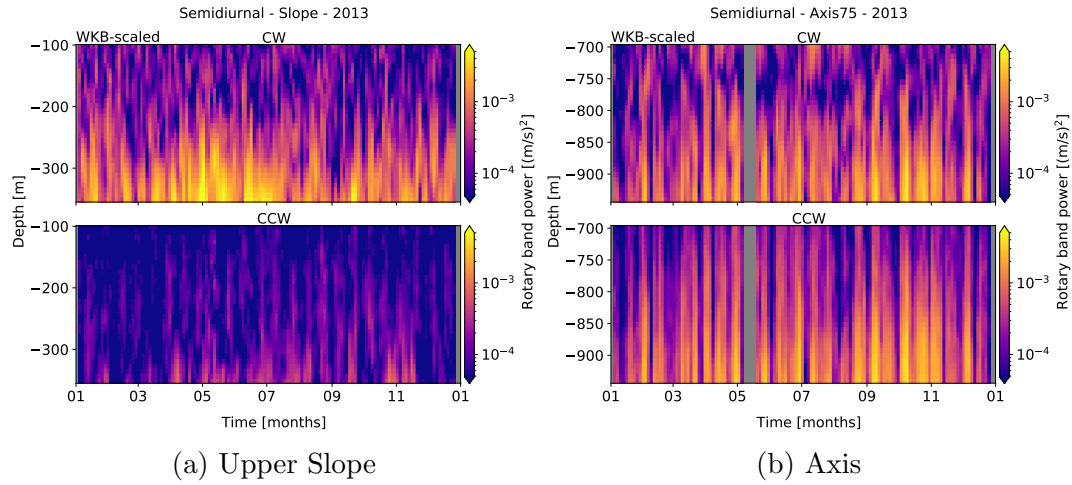


Figure 6: Integrated semidiurnal depth-band rotary PSD for (a) Upper Slope and (b) Axis, from horizontal velocity data in 2013.

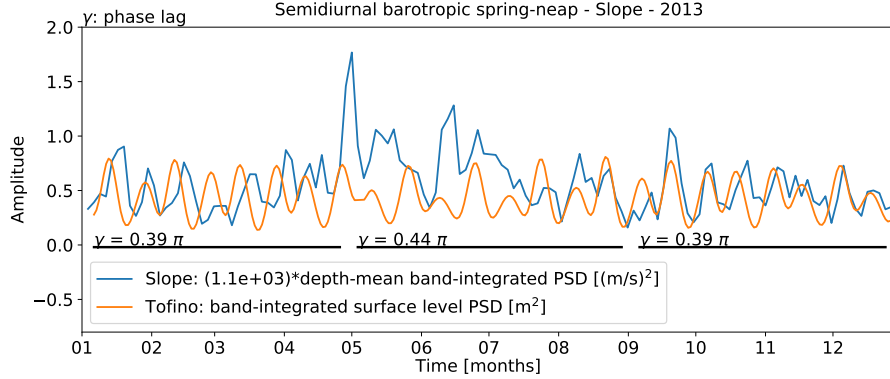
At Upper Slope, semidiurnal seasonality shows a pulse of about half an order of magnitude in the near-topography intensification, in the late-spring through the summer.

At Axis, seasonality is apparently absent.

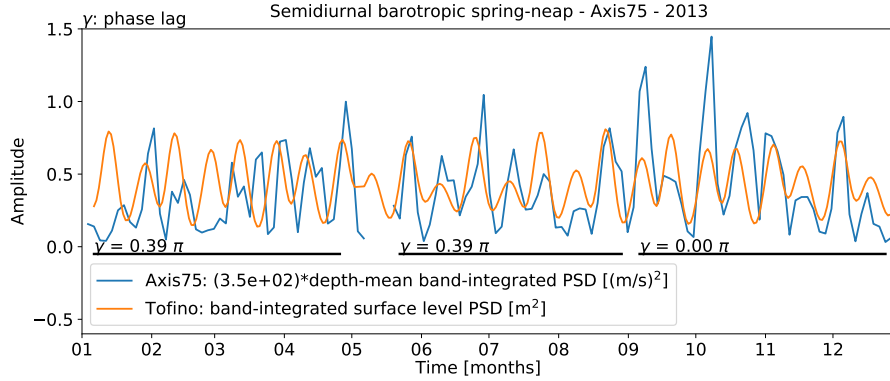
There is fortnightly periodicity at both sites.

To compare this periodicity with likely tidal forcing, the depth-band integrated power plots were depth-averaged at each time step. This was then plotted against similarly processed surface level observations from the Tofino CHS buoy, north of Barkley Canyon, over the same year (Figure 7).





(a) Upper Slope



(b) Axis

Figure 7: Barotropic comparison for (a) Upper Slope and (b) Axis, from horizontal velocity data in 2013. The depth-average of the integrated semidiurnal power (blue) is scaled to compare with the band-passed power of the Tofino surface levels (orange).

Scaled amplitudes vary greatly, with a notable increase at Upper Slope in the late-spring through summer.

Much of the year shows similar timing to the barotropic semidiurnal forcing, but the spring shows a timing offset of 3-4 days, averaged over the five largest gaps in spring, each year.

Correlated phase lag confirms that the tidal forcing is remote, throughout the year, and that this effect is also present in the canyon.

Regional mode 1 wave speed  $c_1$  (Chelton, 1998) is between 2.0 - 2.4 m/s (average 2.2 m/s), depending on distance from Vancouver Island, with minimal seasonal variation below the mixed layer. For the generalised offsets deter-

mined, this suggests a mode 1 travel distance of 700 - 800 km.

## **2 Comparisons**

XXX

## **3 Speculation**

XXX

## **4 Discussion**

XXX

## 5 References

XXX